NAVIER STOKES ANALYSIS OF LOW ASPECT RATIO RECTANGULAR FLAT WINGS IN COMPRESSIBLE FLOW

ICAS-94-10.4.3

Figen Laçin[1] and Mehmet Şerif Kavsaoğlu[2]
Middle East Technical University, Department of Aeronautical Engineering
06531 Ankara, TURKEY

Abstract

Flowfield of an aspect ratio 1 sharp edged rectangular flat plate wing placed in subsonic compressible flow was analyzed by the solution of three dimensional, thin layer, compressible Navier Stokes equations. A single block grid of about 100000 points was generated. A finite difference solution algorithm (LANS3D) with LU-ADI decomposition was used and Baldwin Lomax turbulence model was applied.

Introduction

Low aspect ratio ractangular flat wings are in general used in missiles. Some of the missiles which are donated with these wings fly and manouver at high angles of attacks. General description of the flowfields of these wings can be seen in Figure 1. Flow separates at the sharp leading edge and forms the leading edge bubble. There are also two side edge vortices which are similar to the leading edge vortices of Delta wings. In general missile aerodynamics and high angle of attack aerodynamics are dominated with vortical and separated flows. Various publications by AGARD provide a large selection of research results in these fields[1-6]. Investigation of these publications show that majority of the earlier research results were experimental which may be attributed to the three dimensional and seperated nature of the flowfields. By the development of three dimensional Navier-Stokes solvers more and more computational results are becoming available[4].

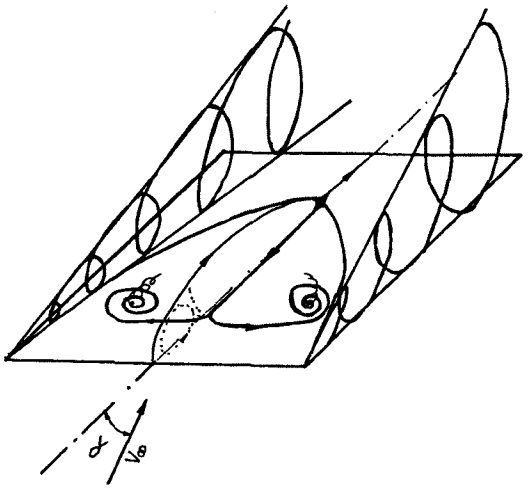

Figure 1. General description of the flowfield[10].

Low aspect ratio rectangular flat wings were studied much less when compared to the Delta wings of the similar nature. Stahl[7] summarized some of the early research works. Winter[8] obtained pressure distributions on the suction side and force and moment measurements of various low aspect ratio rectangular flat wings at incompressible speeds. At von Karman Institute similar experiments were performed in a transonic wind tunnel for higher speeds[9-10]. In Figures 2, 3 and 4 sample pressure distribution, force measurement and flow visualisation results from these experiments can be seen.

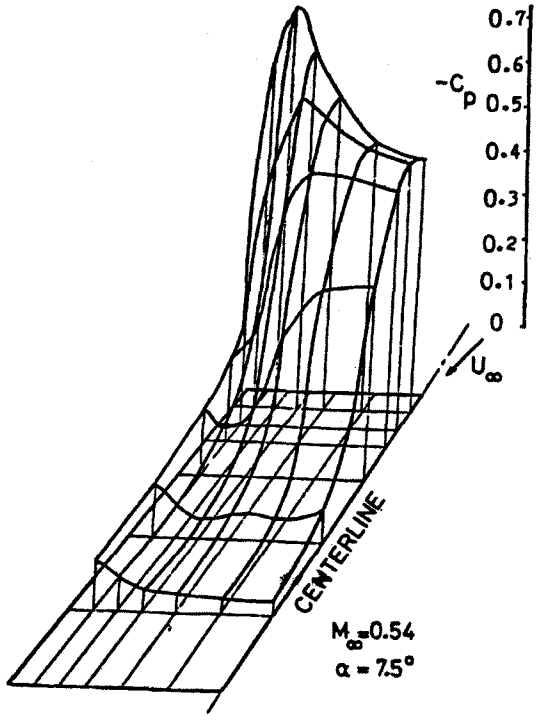

Figure 2. Pressure distribution on the suction side of an aspect ratio 1 rectangular flat plate[9], α = 7.5, Mach = 0.54, Re_c = 3e5.

In the present study the experiments of van Westerhoven *et. al*[9]. and Kavsaoğlu[10] was taken as test cases for comparison of the results. The flowfield of an aspect ratio 1 flat plate was analysed by using a three dimensional, thin layer, compressible Navier Stokes solver (LANS3D)[11,12] at various angles of attack and Mach numbers. A single block grid of about 100,000 points was used. This grid was a half grid due to

[1] Graduate Student.
[2] Associate Professor, Member AIAA.

symmetry of the flowfield. Baldwin-Lomax[13] turbulence model was used.

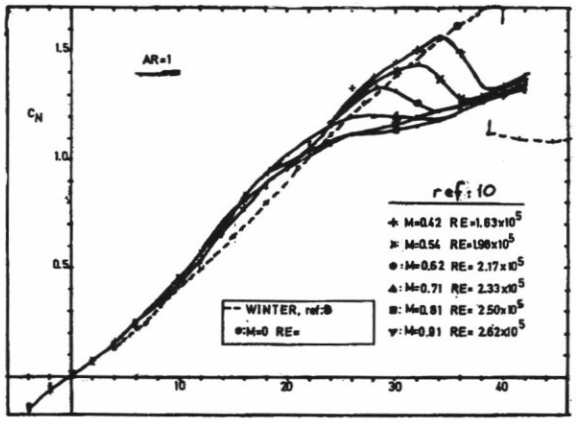

Figure 3. Normal Force measurements of an aspect ratio 1 rectangular flat plate[8, 10].

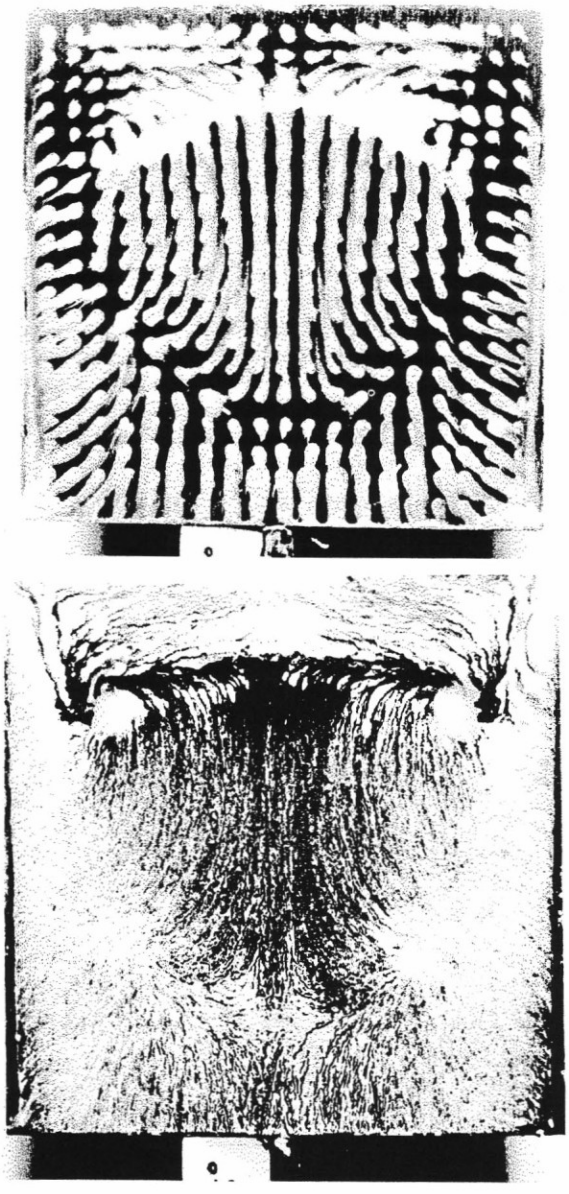

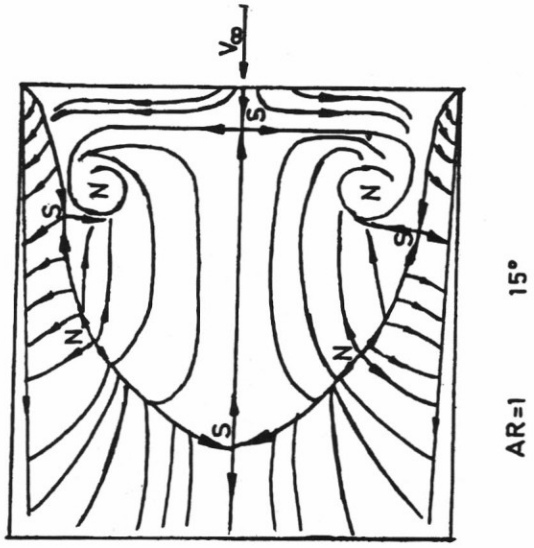

Figure 4. Surface Streamlines of an aspect ratio 1 rectangular flat plate[10], $\alpha = 15^\circ$, Mach = 0.1.

Wing Geometry and Grid

Geometric details of the flat plate wing model are given in Figure 5. The wing aspect ratio is 1 and it has sharp edges. An algebraic grid which wraps around this wing in η direction was produced. Due to the symmetry of the flowfield with respect to the x-z plane this was a half grid. Grid dimensions were JMAX*KMAX*LMAX = 51*43*49 = 107457 points in ξ, η, ζ directions respectively. In η irection K = 2 plane and K = 42 planes lie in the symmetry plane of the wing (y = 0). K = 1 and K = 3 planes are

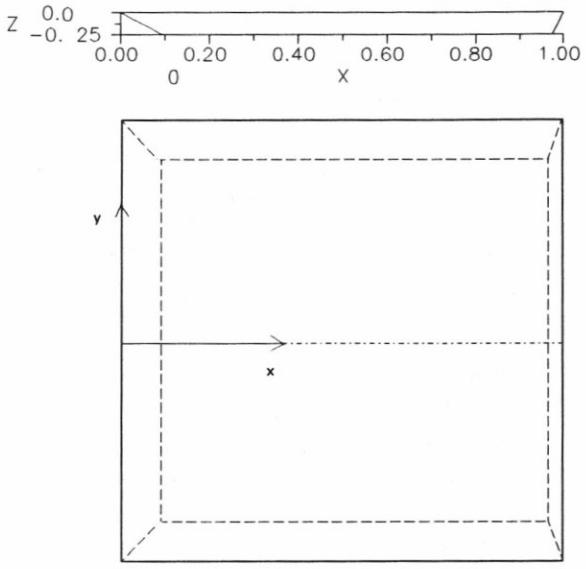

Figure 5. Flat plate wing geometry.

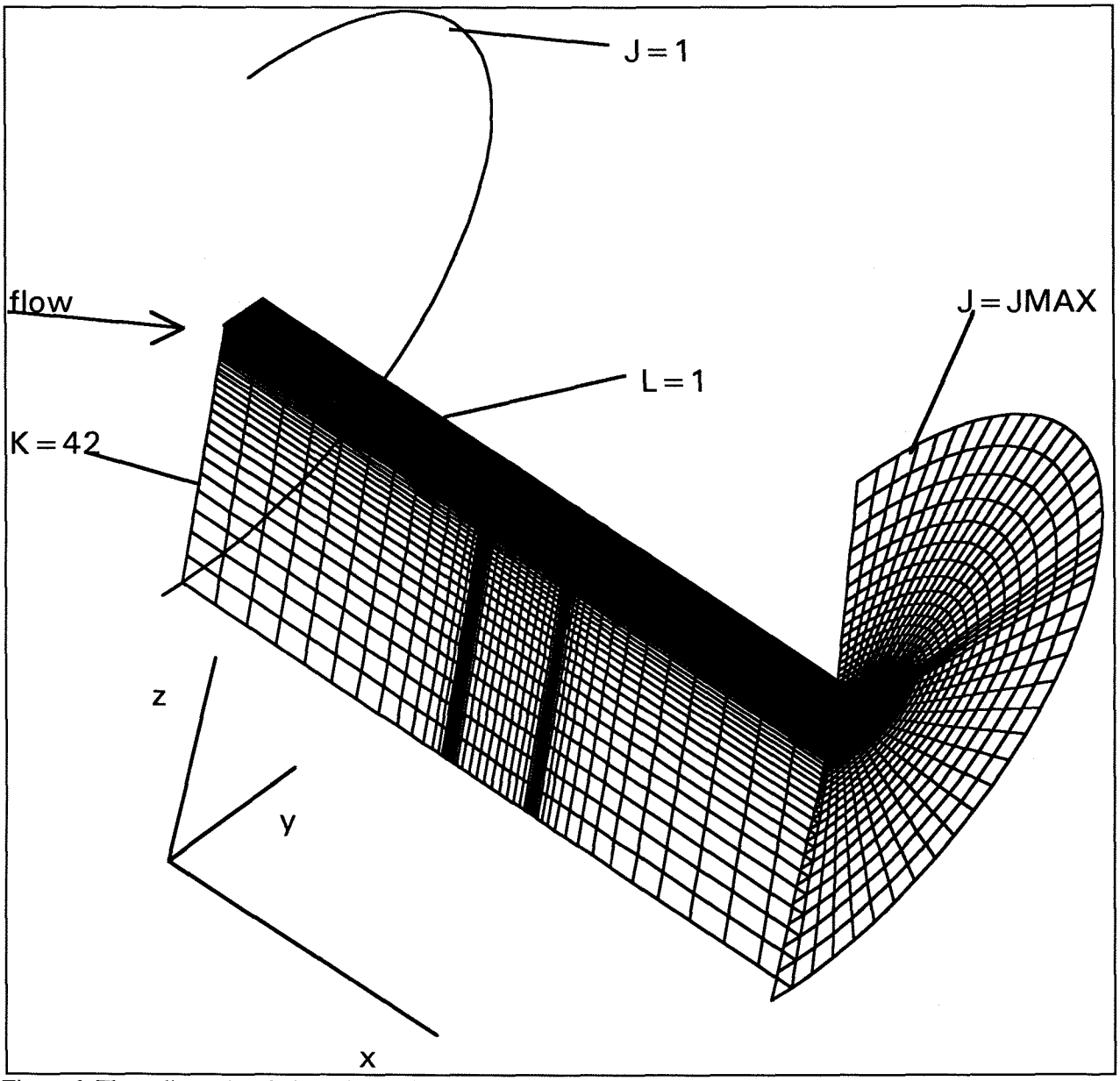

Figure 6. Three dimensional view of the grid.

symmetric with respect to K=2 plane and K=41 and K=43 planes are symmetric with respect to K=42 plane for ease of specifying symmetry boundary conditions. On model surface (L=1) K=21, 22 and 23 lines coincide at the wing side edge forming a singular line.

In ξ direction J=15 corresponds to the leading edge and J=35 corresponds to the trailing edge of the wing at the surface. The grid extends from x/c = -3 to 4, from y/c = 0 to 3.5, and from z/c = -3 to 3. In ζ direction the smallest grid distance from the wing surface was roughly calculated as $1/\sqrt{\mathrm{Re}_c}$. In Figure 6 a three dimensional view of the grid can be seen. In Figure 7 an overall view of the grid in J=25 surface and in Figure 8 an enlarged wiev of this surface around the wing side edge are given. In Figure 9 an enlarged view of the K=2 and K=42 surfaces which both lie in the wing symmetry plane can be seen. In Figure 10 the grid lines on the wing upper surface (partial view of the L=1 surface) are presented.

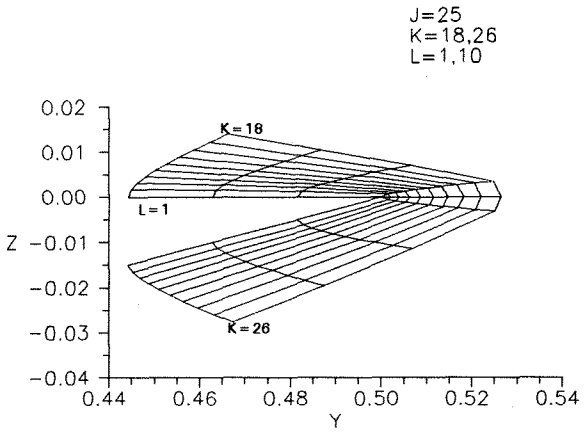

Figure 8. Enlarged view of the J=25 surface.

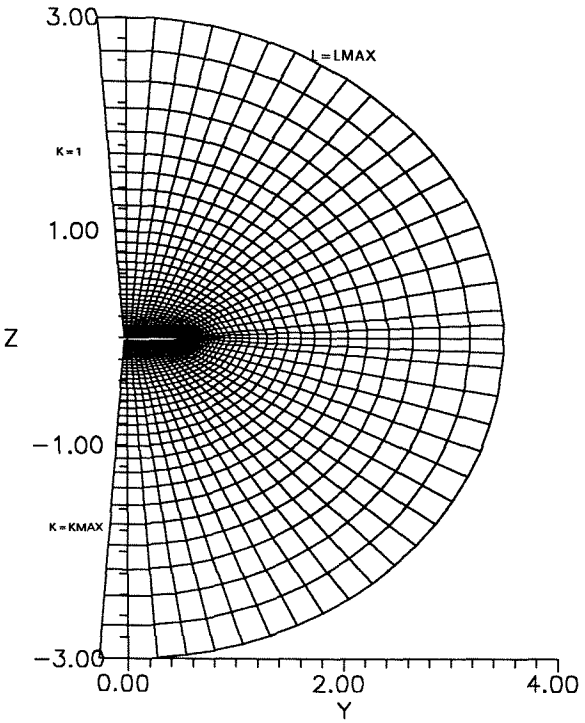

Figure 7. J=25 surface of the grid.

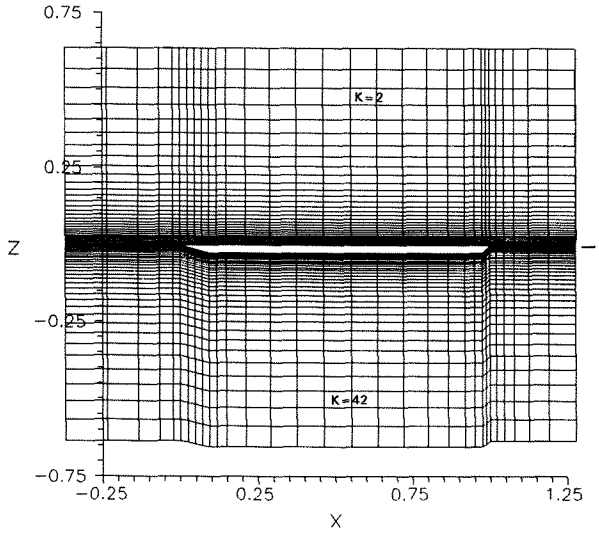

Figure 9. K=2 and K=42 planes of the grid, enlarged around the wing.

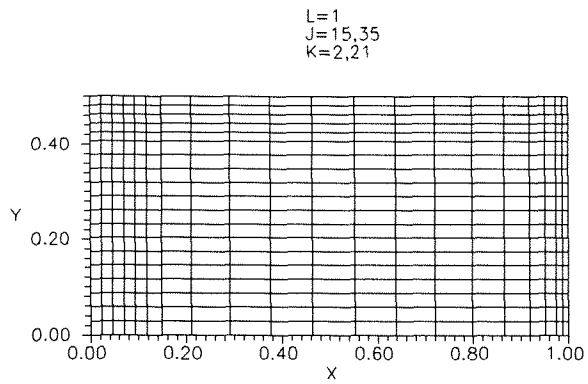

Figure 10. Grid lines on the wing upper surface, L=1, J=15 to 35, K=2 to 21.

Numerical Method

LANS3D[11, 12] algorithm was used for the solution of thin layer, compressible, Reynolds Averaged Navier Stokes equations written in strong conservation form. These equations which are transformed from the (x,y,z,t) cartesian coordinates to the general time dependent curvilinear coordinates { $\tau = t$, $\xi = \xi(x,y,z,t)$, $\eta = \eta(x,y,z,t)$, $\zeta = \zeta(x,y,z,t)$ } read

$$\hat{U}_\tau + \hat{E}_\xi + \hat{F}_\eta + \hat{G}_\zeta = k\hat{S}_\zeta / Re$$

where

$$\hat{U} = J^{-1}\left[\rho,\ \rho u,\ \rho v,\ \rho w,\ e\right]^T$$

is the vector of dependent variables, J is the Jakobian of the transformation, Re is the Reynolds number, $\hat{E}$, $\hat{F}$, $\hat{G}$ are the inviscid flux vectors and $\hat{S}$ is the thin layer viscous flux vector. k=1 for viscous flows and k=0 for inviscid flows. Complete description of the thin layer equations are documented in Ref. 12. LANS3D program uses an LU-ADI factorization algorithm with diagonally dominant LU factorization[11, 12].

Boundary Conditions

At the upstream infinity (J = 1 plane) and at the outer edge of the grid (L=LMAX surface) freestream conditions were specified:

$\rho = \rho_\infty$, $u = U_\infty \cos\alpha$, $v = 0$, $w = U_\infty \sin\alpha$, $p = p_\infty$

then, energy can be calculated from:

$$e = \frac{p}{\gamma - 1} + \frac{1}{2}\rho(u^2 + v^2 + w^2)$$

At the flow exit plane (J=JMAX plane) pressure was fixed to the freestream value ($p = p_\infty$) and other variables (ρ, u, v, w) were extrapolated from the J = JMAX - 1 plane. Since the flowfield is symmetric with respect to the y = 0 plane symmetry boundary conditions were utilized. As explained above, K = 2 plane and K = 42 planes lie in the symmetry plane (y = 0) and K = 1 and K = 3 surfaces are symmetric with respect to K = 2 plane and K = 41 and K = 43 (KMAX) surfaces are symmetric with respect K = 42 plane. Then the boundary conditions for K = 1 and K = KMAX planes were specified as follows:

$\rho_1 = \rho_3$ $\quad \rho_{KMAX} = \rho_{KMAX-2}$

$u_1 = u_3$ $\quad u_{KMAX} = u_{KMAX-2}$

$v_1 = -v_3$ $\quad v_{KMAX} = -v_{KMAX-2}$

$w_1 = w_3$ $\quad w_{KMAX} = w_{KMAX-2}$

$e_1 = e_3$ $\quad e_{KMAX} = e_{KMAX-2}$

L = 1 surface from J = 15 to 35 corresponds to flat plate wing surface. J = 15 is the leading edge and J = 35 is the trailing edge. From K = 1 to 21 upper surface, from K = 23 to KMAX lower surface was defined. At the side edge of the wing K = 21, 22, and 23 lines coincide forming a singular line. On the flat wing surface (L=1) no slip condition was specified by u = v = w = 0, pressure was taken from the L=2 surface and density was extrapolated from L=2 and L=3 surfaces. For the part of the L=1 surface which is not in contact with the wing surface the points from K=1 to 20 coincides with the points from K=43 to 24. For example K=3 and K=41 coincides and they have the same density, velocity and pressure values. These variables were assigned by averaging the corresponding values from the K=3, L=2 and K=41, L=2 points. For the three singular lines of the L=1 surface (K=21, 22 and 23) density, velocity components and pressure values are assigned as the averaged values of the K= 21, 22, and 23 line values of the L=2 surface.

Computational Details

Baldwin Lomax[13] turbulence model was applied starting from the wing leading edge for the viscous region around the wing. It also worked in the wake region behind the wing. Jacobian and metric values of the singular lines (L=1, K=21, 22 and 23) were assigned from the corresponding points of the L=2 line. Computations were performed on the IBM 3090 180S vector machine with single CPU installed at the Middle East Technical University. About 40 megabytes of RAM needed for 51*43*49 grid points and 1000 iteration lasted about 3 hours and 59 minutes CPU time including one read and one write operation of the solution file and one read operation of the grid file.

Results

In Figure 11. a typical convergence history of the iterations is presented. Upper curve represents the L2 norn of residual and lower curve represents the maximum local residual. In Figure 12. convergence of the centerline pressures on the wing upper surface is presented. It seems like about 3000 iterations were sufficient for the convergence of the centerline pressures. In Figure 13. the upper surface pressure field prediction is presented for $\alpha = 7.5^{\circ}$,Mach = 0.54

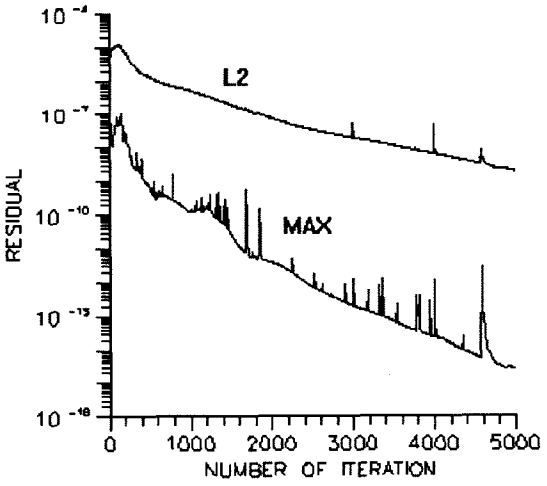

Figure 11. A typical convergence history, α = 7.5° ,Mach = 0.54, Re = 3e5.

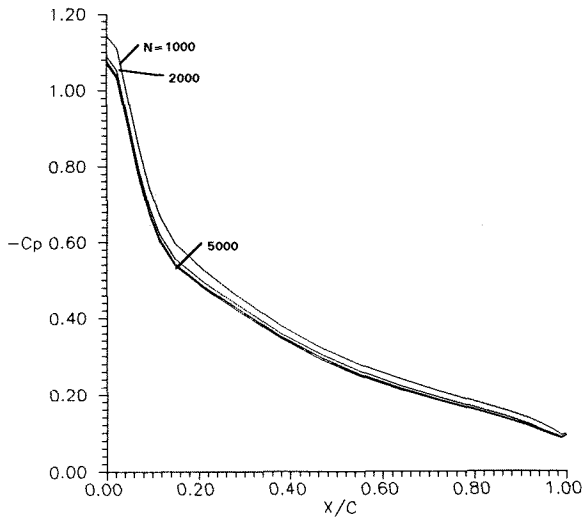

Figure 12. Convergence of the centerline pressure field on the upper surface by the number of iterations, N, α = 7.5° ,Mach = 0.54, Re = 3e5.

and Re=3e5. This result can be compared with the experimental result[9] presented in Figure 2. It seems like the side edge vortices were predicted, however the leading edge buble's prediction was not succesful. This may be because of ignoring the laminar portion of the viscous layer around the leading edge, and/or coarse grid spacings in x direction. In Figures 14., 15. and 16. surface pressure predictions in x direction at 2y/b= 0, 0.64 and 0.88 locations are presented in comparison

with the experimental results[9]. For these figures α = 5.5° Mach = 0.55, and Re_c = 2.6e5.

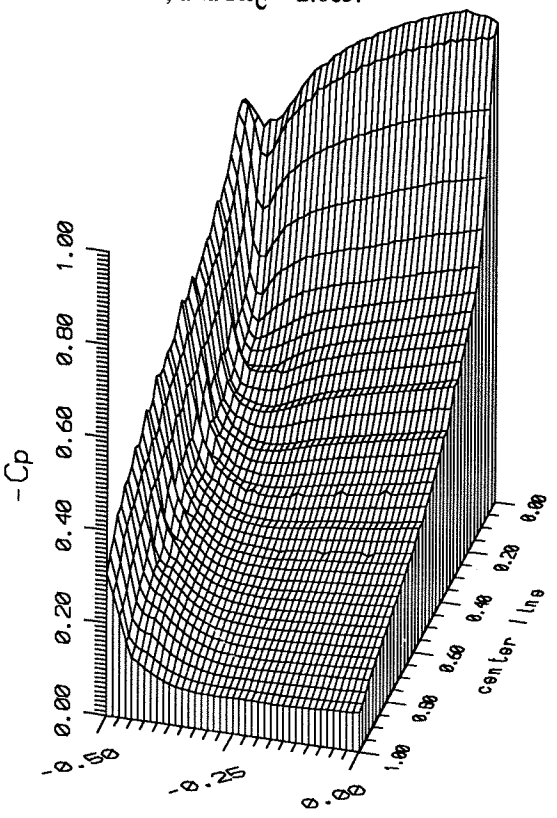

Figure 13. Surface pressures, α = 7.5° ,Mach = 0.54, Re = 3e5.

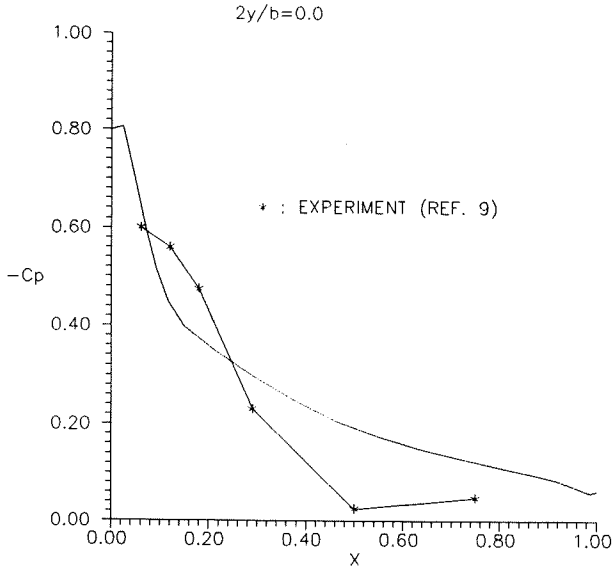

Figure 14. Surface pressures on the upper surface, 2y/b = 0, α = 5.5° Mach = 0.55, Re_c = 2.6e5.

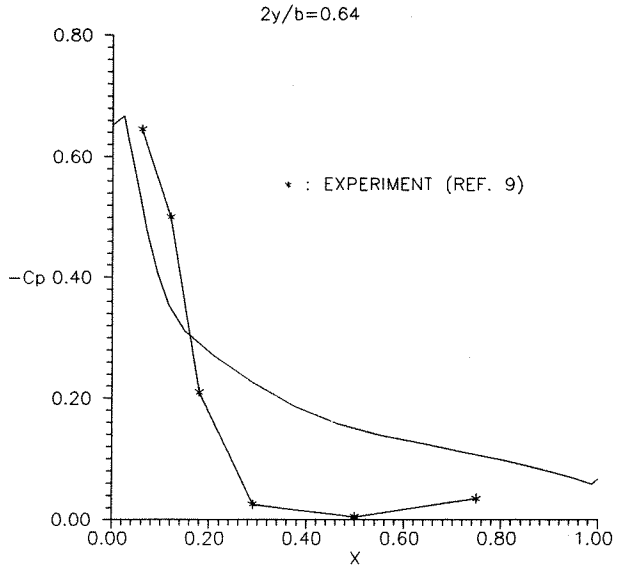

Figure 15. Surface pressures on the upper surface, 2y/b = 0.64, α = 5.5° Mach = 0.55, Re_c = 2.6e5.

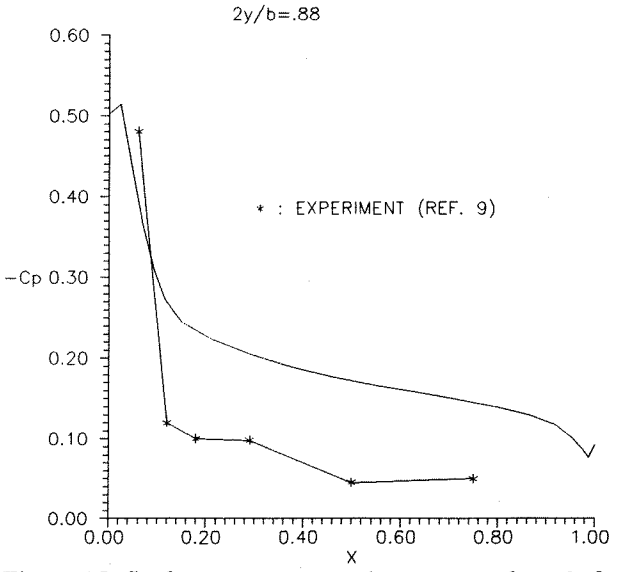

Figure 15. Surface pressures on the upper surface, 2y/b = 0.88, α = 5.5° Mach = 0.55, Re_c = 2.6e5.

Discussion

Preliminary results obtained of the present research are presented. More careful application of the turbulence model, considering the laminar portion of the viscous layer around the wing leading edge may improve the results. The use of Johnson-King[14] turbulence model which was tested by Kaynak *et. al.*[15] for the Navier-Stokes solution of Delta wing flowfields may be considered in a future study. Finer grid spacing in x direction around the leading edge may improve the results. Present research efforts are still continuing. Computation of the cases with various angles of attack, and Mach numbers and comparison of the pressure field, surface streamlines, and force- moment coefficients with the available experimental data were also planned within the present research.

Acknowledgements

During this research the first author received a graduate scholarship from the Scientific and Technical Research Council of Turkey (TUBITAK). She also received a partial travel support for attending the conference from the same organization. The authors would like to thank Kozo Fujii of ISAS-JAPAN and his co-workers for permission to use LANS3D code. Thanks also go to Serkan Şen and Beytullah Temel of TUBITAK-SAGE (Turkey) for their help during the initial stages of the grid generation.

References

1. AGARD CP-247, "High Angle of Attack Aerodynamics", 1979.
2. AGARD LS-98, "Missile Aerodynamics", 1979.
3. AGARD LS-121, "High Angle of Attack Aerodynamics", 1982.
4. AGARD CP-494, "Vortex Flow Aerodynamics", 1991.
5. AGARD CP-497, "Maneuvering Aerodynamics", 1991.
6. AGARD R-776, "Special Course on Aircraft Dynamics at High Angles of Attack: Experiments and Modelling",1992.
7. Stahl W. H., "Aerodynamics of Low Aspect Ratio Wings", in AGARD LS-98, "Missile Aerodynamics", 1979.
8. Winter H., "Strömungsvorgange an Platten und profilierten Körpern bei kleinen Spannweiten. Forsch. Ing. -Wes., Vol. 6, 1935, pp. 40-50, 67-71. Also: "Flow Phenomena on Plates and Airfoils of Short Span", NACA Rep. 798, 1937.
9. van Westerhoven P., Wedemeyer E., Wendt J. F., "Low Aspect Ratio Rectangular Wings at High Incidences", Paper presented at the AGARD Symposium on Missile Aerodynamics, Trondheim, Norway, September 20-22, 1982.
10. Kavsaoğlu M. Ş, "Flow Around Low Aspect Ratio Rectangular Flat Plates Including Compressibility", von Karman Institute For Fluid Dynamics,VKI-PR 1982-15, June 1982.
11. Obayashi S., Matsushima K., Fujii K., and Kuwahara K., "Improvements in Efficiency and Reliability for Navier Stokes Computations Using the LU-ADI Factorization Algorithm", AIAA Paper 86-0338, Jan. 1986.
12. Fujii K. and Obayashi S., "Practical Applications of the New LU-ADI Scheme for the Three-Dimensional Navier-Stokes Computation of Transonic Viscous Flows", AIAA Paper No. 86-0513, Jan. 1986.
13. Baldwin B. S. and Lomax H., "Thin Layer Approximation and Algebraic Model for Separated Turbulent Flows", AIAA Paper No. 78-257, Jan. 1978.
14. Johnson D. A. and King L. S., "A New Turbulence Closure Model forBoundary Layer Flows with Strong Adverse Pressure Gradients and Separation",AIAA Paper 84-0175, 1984.
15. Kaynak Ü., Tu E., Dindar M., and Barlas R., Nonequilibrium Turbulence Modelling Effects on Transonic Vortical Flows About Delta Wings",in AGARD CP-494, "Vortex Flow Aerodynamics", 1991.